Ecological Modelling 221 (2010) 1440–1450

Contents lists available at ScienceDirect

Ecological Modelling

journal homepage: www.elsevier.com/locate/ecolmodel

Predicting future effects from nutrient abatement and climate change on phosphorus concentrations in Lake Bourget, France

Andreas C. Bryhn[a,*], Cyrille Girel[b], Gérard Paolini[b], Stéphan Jacquet[c,*]

[a] Department of Earth Sciences, Uppsala Univ., Villav. 16, 752 36 Uppsala, Sweden
[b] CISALB, 42 rue du pré Demaison, 73000 Chambéry, France
[c] INRA, UMR CARRTEL, 75 avenue de Corzent, 74203 Thonon-les-Bains Cedex, France

ARTICLE INFO

Article history:
Received 16 April 2009
Received in revised form 12 February 2010
Accepted 23 February 2010
Available online 20 March 2010

Keywords:
Phosphorus
Loading
Modelling
Forecasting
Lake
Eutrophication

ABSTRACT

Like many temperate European lakes, Lake Bourget (France) has suffered from eutrophication during the second half of the last century. Due to a remarkable restoration program, the lake has been recovering for the past 25 years after a massive decrease in total phosphorus (TP) loading. TP concentrations have decreased from about 100–120 to 20–25 μg/L. Additional efforts are, however, still required to obtain a perennially sustainable good ecological status and model parameterisation of fluxes can assist in predicting future outcomes, especially in the context of global warming. In this paper, a dynamic model (MeroLakeMab) was developed and tested with the purpose to reconstruct the loading history of Lake Bourget and to predict TP concentrations during scenarios of increased temperature, decreased water runoff and decreased P loading. Simulations suggested that the historical TP loading decrease may have been as extensive as 88%. Decreases in water discharge to Lake Bourget at magnitudes forecasted by the Intergovernmental Panel on Climate Change (IPCC) would not affect TP concentrations notably, but marked concentration changes could, however, occur if decreases in runoff would have a strong impact on the TP loading. Increasing temperature effects on yearly mean TP concentrations in the water column would be very small compared to effects from changes in the TP loading. Predictions such as these could be instrumental for future successful lake management.

1. Introduction

Eutrophication of lakes has been a major environmental concern during recent decades. It has been attributed to increased anthropogenic phosphorus (P) loading to the lakes from domestic sewage, industries and runoff from fertilised agricultural areas, and is manifested as intensified algal or cyanobacterial blooms, decreased visibility in the water, oxygen depleted bottoms, and, in some cases, fish kills (Vollenweider, 1976; Sas, 1989; Chorus and Bartram, 1999; Jeppesen et al., 2005). Recently, Schindler et al. (2008) presented results from a 37-year whole ecosystem experiment which confirmed a commonly held view that eutrophication of most lakes cannot be controlled by nitrogen inputs and that the focus in management must instead be on decreasing P inputs. It is now also well established that many eutrophicated lakes have recovered after significant decreases in P loading (Sas, 1989; Jeppesen et al., 2005). One such example is Lake Bourget, the largest natural lake in France, located in the southern part of the Alps. Although a substantial re-oligotrophication has been observed in this lake after extensive measures to decrease the P loading (Vinçon-Leite et al., 2002), eutrophication is still of great concern to lake managers and residents in the area. The water quality has been intensively surveyed; in the lake since 1981 and in the main tributaries since 2004 (Jacquet et al., 2008). A recent sediment core study showed a particularly pronounced prevalence of large calcite crystals, diatoms, and total organic carbon deposited in the 1980s and 1990s, indicating high internal P loading during this period (Giguet-Covex et al., 2010). Complete mixing of the water column normally occurs in the winter but less frequently than once a year, which means that the lake can be viewed as meromictic (Jacquet et al., 2005; Boehrer and Schultze, 2008).

Phosphorus abatement is often very costly, and one common way to estimate the future response of the water quality and ecosystem interactions of the lake before undertaking costly measures is to use predictive eutrophication models, although the uncertainty in many predictive models may discourage the use of them as a basis for action (Sas, 1989). Furthermore, the possible effects from climate change (i.e., global warming, changes in precipitation and changes in the length of drought periods) on various types of ecosystems have aroused widespread concern in the scientific community and elsewhere (IPCC, 2008). According

* Corresponding authors.
E-mail addresses: andreas.bryhn@geo.uu.se (A.C. Bryhn), stephan.jacquet@thonon.inra.fr, jacquet@thonon.inra.fr (S. Jacquet).

0304-3800/$ – see front matter © 2010 Elsevier B.V. All rights reserved.
doi:10.1016/j.ecolmodel.2010.02.013

Nomenclature

A	area
Area	lake surface area
C	concentration
CV	coefficient of variation
D_{crit}	critical depth
D_m	mean depth
D_{max}	maximum depth
Deep A	deep accumulation sediments
diff	diffusion
DR	dynamic ratio
DW	deep waters
ET	erosion and transport sediments
F	phosphorus flux
IPCC	Intergovernmental Panel on Climate Change
Lat	latitude
MidA	mid-range accumulation sediments
mix	mixing
MW	middle waters
P	phosphorus
PF	particulate fraction
Prec	precipitation
R	rate
Q	water flux
sed	sedimentation
SW	surface waters
TP	total phosphorus
V	volume
V_d	volume development
Y	dimensionless moderator

to the A1B climate change scenario (200–300% increase in carbon dioxide emissions from year 1990 to 2100), runoff in the catchment area of Lake Bourget could decrease by about 10–20% until 2080–2099 (IPCC, 2007, 2008). Three climate scenarios (A2, A1B and B1; 0–600% increase in carbon dioxide emissions from 1990 to 2100) all indicate average temperature increases on the earth surface in south-eastern France, by up to 4.5 °C (IPCC, 2007).

Many previously published load–concentration models are unable to predict future P concentrations in meromictic lakes, for reasons which will be discussed in the following section. Therefore, MeroLakeMab, a dynamic model for deep alpine lakes, will be presented and tested against available data from Lake Bourget and the northern basin of Lake Lugano (Italy/Switzerland; Barbieri and Simona, 2001). Predictions will be compared to those made with LakeMab (a similar model suited for holomictic lakes; Håkanson and Bryhn, 2008) and the widely used Vollenweider model (Vollenweider, 1976).

All dynamic models contain many calibration constants, and calibration can be done more or less arbitrarily—different constant sets can give similar descriptions of the prevailing conditions, a phenomenon known as equifinality (Beven, 2006). The number of possible calibration constant sets decreases drastically if the same model is tested for more than one system without re-calibration (Bryhn and Håkanson, 2007). Moreover, there were only five years (2004–2008) for which both TP concentration data and reliable TP loading data were available regarding Lake Bourget. By testing MeroLakeMab with a fixed set of algorithms and calibration constants against data from two lakes (Lake Bourget and Lake Lugano) instead of one, model predictions may be regarded as more reliable than if the calibration constant set would be valid for one lake only.

After output data from MeroLakeMab have been compared with field measurements (hereafter referred to as "empirical data") from monitoring programmes, the model will be used for reconstructing the loading history to Lake Bourget as well as for predicting total phosphorus (TP) concentrations in this lake during scenarios of increased temperature, decreased water runoff and decreased P loading. Such predictions should be essential for successful management of algal bloom intensity and water clarity in the lake.

Table 1
Geographical and morphological information about the two lakes used for model development.

Lake name	Bourget	Lugano (N. basin)
Latitude, longitude	45°44'N, 5°52'E	46°0'N, 9°0'E
Altitude (Alt)	231 masl	271 masl
Lake area (Area)	44.5 km^2	27.5 km^2
Mean depth (D_m)	80 m	171 m
Max depth (D_{max})	147 m	288 m
Drainage area	560 km^2	269.7 km^2
Water residence time	8.5 years	12.3 years

Table 2
Tributary inflow (Q) and TP load to Lake Bourget from 2004 to 2008. Minor tributaries contributed with a maximum of 6–7 tons TP per year while the remaining part was transported by Rivers Leysse and Sierroz.

Year	Q (10^6 m^3)	TP load (tons)
2004	240	47–48
2005	220	27–28
2006	240	25
2007	380	33
2008	330	18

2. Materials and methods

2.1. Study areas

MeroLakeMab was developed for conditions in the northern basin of Lake Lugano as described by Barbieri and Simona (2001) and for conditions in Lake Bourget 2004–2007 described in the present study. Additional data for Lake Bourget were collected during the calibration process in 2008. Basic data about the two lakes used for model development and testing are given in Table 1. TP loading, TP concentrations and water budget data for Lake Lugano were taken from Barbieri and Simona (2001). The total tributary TP loading and water inflow (Q) for Lake Bourget 2004–2008 (earlier loading data were either insufficient or based on estimates) are given in Table 2. The two main tributaries are the River Leysse and the River Sierroz (responsible for about 80% of the water inflow), while the three smaller tributaries are Tillet, Belle-Eau and Grand Canal (no data available) and also for a few days during the year the Savières channel (i.e. the only outflow from the lake which also contributes to <1% of the annual water inflow; Jacquet et al., 2008).

2.2. Models

There is a wide variety of eutrophication models available, the oldest ones being based on one or a few equations and yielding rather uncertain predictions (Sas, 1989). Although easy to use, these static models do not account for year-to-year variations in internal loading (nutrient transport from sediments to water through resuspension, bioturbation and diffusion) and may therefore comparatively poorly describe the recovery process of eutrophicated lakes (Bryhn and Håkanson, 2007). One well-known and widely used static model that will be tested in this work is that of Vollenweider (1976), which calculates TP concentrations in lakes from two parameters; the TP concentration in the inflowing water and the water retention time.

Another model type is lake-specific and dynamic (i.e. time-dependent). Models in this category (of which there are several sub-types) are more complex than static models; they are based on differential equations to account for processes such as the internal loading, and they include lake-specific calibration constants. However, many of them (e.g., Vinçon-Leite et al., 2002; Pers, 2005; Hu et al., 2006) are driven by meteorological data, which can only be forecasted for a few days ahead, while eutrophication management typically depends on which environmental effects can be expected within the next year, decade, or decades. Furthermore, such models are calibrated and validated for site-specific conditions for which data must be available. The validity of their calibration constant matrix is thus rather limited and does not stretch towards TP loading conditions that differ greatly from those described by validation data. Lake-specific models may be good for descriptive purposes but because of their data requirements and their limited range of validity, they may fail to accurately predict future TP concentration changes and they are also poorly suited for reconstructing reliable TP loading histories.

A third model type also produces dynamic predictions, but is, in addition, general, meaning that the model has been developed to contain a unique and generic set of equations and calibration constants, and the output data have subsequently been tested against empirical data on TP concentrations from several lakes (Aldenberg et al., 1995; Janse, 2005; Bryhn and Håkanson, 2007; Håkanson and Bryhn, 2008). Only easily accessible and measurable driving variables are used (e.g., lake area, mean and maximum depth and total P loading) and driving variable values should be site-specific for each lake. No meteorological data or other scarcely predictable data (on the annual or multiannual scale) are used as driving variables. There are at least two general TP models available; PCLake, whose output data have been tested against data from shallow European lakes (Janse, 2005), and LakeMab, which has been tested against TP data from deep and shallow lakes from northern Sweden to central Florida (Bryhn and Håkanson, 2007). However, neither of these models has been tested against data from meromictic lakes, which for long periods sustain three vertical water layers with limited exchange of water and P. PCLake simulates P masses and fluxes to and from a mixed water column (Janse, 2005) while LakeMab describes two communicating vertical water layers.

The model developed in this study is referred to as MeroLakeMab. It is based on LakeMab (Håkanson and Bryhn, 2008), but has been expanded to predict concentrations and fluxes in three different water layers instead of two layers. The time step (one month) and the length of predictions are equal in the two models. The depths at which the three water layers are typically separated, D_{crit1} and D_{crit2} (the critical depths, in m) are determined by means of two statistical models which are based on multi-lake surveys described by Håkanson et al. (2004) and Bryhn (2009). These two statistical models are defined as

$$D_{crit1} = \frac{45.7 \cdot \sqrt{(\text{Area} \cdot 10^{-6})}}{(21.4 + \sqrt{(\text{Area} \cdot 10^{-6})})} \quad (1)$$

$$D_{crit2} = \frac{6.70 \cdot D_{max}^{1.23}}{(21.4 + \sqrt{(\text{Area} \cdot 10^{-6})})} \quad (2)$$

where D_{max} is the maximum depth (in m) and area is the lake surface area (in m^2; Håkanson et al., 2004; Bryhn, 2009). It should be noted that the constants 45.7 and 21.4 in Eq. (1) and the constant 21.4 in Eq. (2) have the dimension [m] while the first constant in Eq. (2) (6.70) has the dimension [$m^{0.77}$]. Empirical measurements of D_{crit1} and D_{crit2} often show great areal and temporal variability in each lake (Håkanson et al., 2004; Bryhn, 2009), so Eqs. (1) and (2) are particularly well-suited for nutrient modelling on monthly or yearly time scales using general model structures. The division of water layers and bottom areas according to vertical position in relation to the critical depths is illustrated in Fig. 1. Shallow sediments above D_{crit1} are referred to as erosion- and transport-sediments and are highly exposed to wind and wave action so this is where sediment resuspension mainly occurs in a lake (Håkanson and Peters, 1995; Håkanson et al., 2004). Below D_{crit1}, sediments are instead mainly exposed to processes such as particle accumulation, sediment burial and dissolved P diffusion. The higher the temperature, sedimentation or TP content, the more intensive the P diffusion (see Appendix A or Håkanson and Bryhn, 2008). ET, the dimensionless ratio of areal distribution of erosion- and transport-sediments to the lake surface area, was calculated using an algorithm from Håkanson and Bryhn (2008):

$$\text{ET} = \frac{1 - (D_{max} - D_{crit1})}{(D_{max} + D_{crit1} \cdot e^{(3 - V_d 1.5))^{(0.5/V_d)}}} \quad (3)$$

where V_d is the volume development; a (dimensionless) mean depth (D_m) to D_{max} ratio which describes the shape of the hypsographic (cumulative area) curve (Håkanson and Peters, 1995). There are additional boundary conditions (see Appendix A) that limit ET to remain between 0.15 and 0.95. Analogously with Eq. (3), MidA, the algorithm for the dimensionless ratio of accumulation bottom areas between D_{crit1} and D_{crit2} to the total lake area, was calculated as

$$\text{MidA} = \frac{1 - (D_{max} - D_{crit2})}{(D_{max} + D_{crit2} \cdot e^{(3 - V_d 1.5))^{(0.5/V_d)}} - \text{ET}} \quad (4)$$

Finally, DeepA, the dimensionless ratio of accumulation bottom areas below D_{crit2} to total lake area is:

$$\text{DeepA} = 1 - \text{ET} - \text{MidA} \quad (5)$$

The volume of surface waters (SW; epilimnion), V_{SW} (in m^3), was calculated according to Håkanson and Bryhn (2008):

$$V_{SW} = \text{Area} \cdot \left(\frac{D_m - (\text{MidA} + \text{DeepA}) \cdot V_d \cdot (D_{max} - D_{crit1})}{3} \right) \quad (6)$$

Analogously, the volume of deep waters (DW; monimolimnion), V_{DW} (in m^3), is given by:

$$V_{DW} = \text{Area} \cdot \frac{A_{DW} \cdot V_d \cdot (D_{max} - D_{crit2})}{3} \quad (7)$$

The middle water layer (MW; mixolimnion) volume, V_{MW} (in m^3), was then calculated as:

$$V_{MW} = \text{Area} \cdot D_m - V_{SW} - V_{DW} \quad (8)$$

Subscripts SW, MW, and DW used in Eqs. (6)–(8) and elsewhere in this study refer to surface waters, middle waters and deep waters, respectively, as depicted in Fig. 1. The criteria for developing MeroLakeMab were the following:

- The structure should be as simple as possible and should to the greatest extent possible replicate LakeMab, whose detailed test

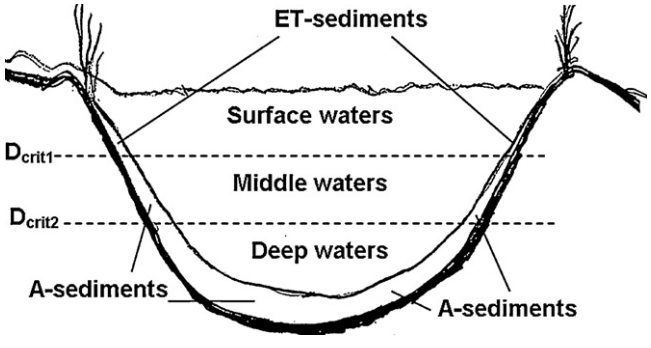

Fig. 1. The vertical distribution of bottom types, water layers and critical depths used in MeroLakeMab. Not to scale.

results (r^2 = 0.96 for modelled TP concentrations against empirical data in a cross-systems comparison) have been reported in Bryhn and Håkanson (2007) and Håkanson and Bryhn (2008).
- TP concentrations should be predicted as accurately as possible in both lakes.
- TP concentrations in the top 10 cm of accumulation area sediments should not exceed 2 mg/g dw (Håkanson and Bryhn, 2008) and not be lower than 0.4 mg/g dw, which is the lower end of the empirical data range from Lake Bourget.
- The particulate fraction (PF); i.e., the ratio of particulate to total phosphorus, should be near 0.6 and within the range of 0.25–0.86 (Bryhn et al., 2007).
- All constants and equations should be identical for both lakes.
- The obligatory driving variables (see below) should be lake-specific.

The use of identical constants and equations for both lakes could decrease the arbitrariness in the calibration process and model structure. Different combinations of equations and constants can produce similar output data (Beven, 2006), so an important aim in generalised lake modelling is to single out the combination of equations and constants which gives the most credible description of several systems (Bryhn and Håkanson, 2007). The eight driving variables used for MeroLakeMab and LakeMab were *Q*, TP load, Alt (altitude, m.a.s.l.), area, D_{max}, D_m, Lat (latitude, °N) and Prec (mean annual precipitation, mm) while only *Q*, TP load, area and D_m were used to make predictions with the Vollenweider model. Alt and Lat are used in LakeMab and MeroLakeMab to estimate water temperatures, the seasonal pattern in tributary discharge, the duration of the growing season, and sedimentation rates. Predictions were compared to yearly mean TP values including coefficients of variation (CV = standard deviation/mean value). Monthly or weekly predictions were not tested due to the scarcity of empirical data. Empirical CVs were calculated where data availability allowed this, but for TP data where standard deviations were not available, CV = 35% was used, which is a typical CV value for TP in lakes on both monthly and annual scales (Håkanson and Peters, 1995). The 95% confidence level was used in all statistical calculations.

3. Results

3.1. Model structure

Fig. 2A shows D_{crit1} in relation to the temperature gradient in Lake Bourget, 1984–2006. Temperatures were rarely below 10 °C in surface waters above D_{crit1} (11 m) and rarely above 20 °C below D_{crit1}. Fig. 2B displays mean TP concentrations at various depths during the period 1999–2008 and clearly shows that there was no apparent TP gradient at D_{crit1} while a strong TP gradient could be found at D_{crit2} (111 m). The presence of a thermocline near D_{crit1} in Fig. 2A and a chemocline near D_{crit2} in Fig. 2B indicates that the division lines according to critical depths (Eqs. (1) and (2)) would be acceptable for TP modelling in this lake. The DW temperature 1984–2006 (see Fig. 2A) showed low variability along the depth gradient, at 5.6 °C (standard deviation 0.4 °C, mean value error 0.13%), so this value was used in the model as the DW temperature. At 115 m, the mean value was 5.7 °C (standard deviation 0.3 °C) while at 140 m, the mean temperature was 5.6 °C (standard deviation 0.4 °C).

The algorithm for net diffusive P transport from bottom waters to middle waters (F_{DWMW}) was as follows:

$$F_{DWMW} = \text{if } (C_{DW} \cdot (1 - PF_{DW}) < C_{MW} \cdot (1 - PF_{MW})) \text{ then } (0) \text{ else } (M_{DW} \cdot R_{diff,DWMW} \cdot (C_{DW} \cdot (1 - PF_{DW}) - (TP_{MW} \cdot (1 - PF_{MW}))) \quad (9)$$

where *C* denotes TP concentrations (in μg/l), and M_{DW} is the TP mass in DW (in g) while MW and DW in subscript indicate middle and bottom waters, respectively. $R_{diff,DWMW}$ was calibrated to 0.008 to match empirical TP concentrations in both lakes. Thus, the net diffusive P transport was assumed to be a function of the difference in concentrations of dissolved P between bottom waters and middle waters. This difference was never lower than 0, so no algorithm for net diffusive P transport in the other direction was needed. The particulate fractions (see Section 2.2) PF_{SW}, PF_{MW} and PF_{DW} were calibrated to 0.6, 0.5 and 0.3, respectively, in order to sustain concentrations in the different water layers of the two lakes which corresponded to empirical measurements. The deep water retention time (T_{DW}; in months) was calculated using F_{DWMW} as a proxy for water flux from deep waters to middle waters:

$$T_{DW} = \frac{M_{DW}}{(F_{DWMW} + 0.001)} \quad (10)$$

The term 0.001 was added in order to avoid division by zero in Eq. (10). The middle water retention time (T_{MW}, in months) was calculated from V_{MW}, the water retention time in the whole lake (*T*, in years) and the water flux from SW to MW (Q_{SWMW}, in m^3/month):

$$T_{MW} = \text{if } \left(\frac{V_{MW}}{Q_{SWMW}} > T \cdot \frac{12}{4}\right) \text{ then } \left(T \cdot \frac{12}{4}\right) \text{ else if } \left(\frac{V_{MW}}{Q_{SWMW}} < 0.5\right) \text{ then } (0.5) \text{ else } \left(\frac{V_{MW}}{Q_{SWMW}}\right) \quad (11)$$

T_{MW} thus had a lower boundary condition of 0.5 months from Håkanson and Bryhn (2008) and *T* converted to months and divided by four was added as an upper boundary condition for T_{MW}.

The sedimentation algorithms in Håkanson and Bryhn (2008) have not been adequately tested for meromictic lakes with low turbulence which may be assumed to provide particularly calm and favourable conditions for sedimentation. To correctly describe the difference in sedimentation and TP retention between the two investigated lakes, a dimensionless moderator ($Y_{DR,sed}$) that affected the sedimentation rate was, in the present study, multiplied with all of the sedimentation flux algorithms ($R_{sed,SW}$, $R_{sed,MW}$, $R_{sed,DW}$; see Appendix A):

$$Y_{DR,\,sed} = 5.8 \cdot \sqrt{DR} \quad (12)$$

where DR is the dynamic ratio (dimensionless; see Appendix A). The rate regarding wind- and wave-driven mixing of the two upper water layers (R_{mix}) in Håkanson and Bryhn (2008) yielded much too high modelled TP_{SW} values and much too low TP_{MW} values in the two meromictic lakes. Instead of letting R_{mix} depend on temperatures, as in Håkanson and Bryhn (2008), R_{mix} was calibrated to 0.00008 $months^{-1}$ which allowed a realistic distinction between TP concentrations in SW and MW in both lakes.

Except for all details mentioned thus far, the rest of the model structure from Håkanson and Bryhn (2008) was kept and the full list of equations is provided in Appendix A. It is worth noting that equations concerning deep waters (DW) in Håkanson and Bryhn (2008) correspond to equations for middle waters (MW) in this work, and A-sediments in Håkanson and Bryhn (2008) correspond to middle water accumulation (MidA) sediments. Algorithms regarding burial, sedimentation and diffusion to or from DW and deep accumulation (DeepA) sediments in this work have been constructed from the corresponding well-tested algorithms regarding the MW layer and MidA sediments in Håkanson and Bryhn (2008).

3.2. Model results versus empirical data

Fig. 3 compares modelled and empirical TP concentrations in Lake Bourget 2004–2008 (a period for which detailed concentration

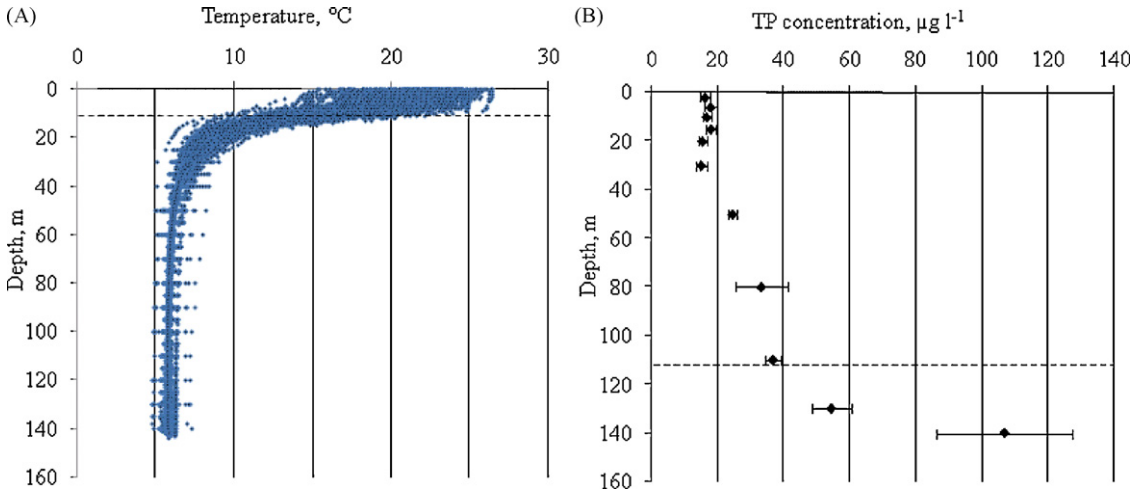

Fig. 2. Temperatures and total phosphorus concentrations at various depths in Lake Bourget. (A) Temperatures 1984–2006. (B) Mean total phosphorus concentrations during the period 1999–2008. Bars represent mean value errors. Dashed lines mark D_{crit1} and D_{crit2}.

data and detailed loading data were both available). For TP in the whole water column, a lake-typical CV value of 0.35 was used to construct uncertainty bands, while annual CVs for SW, MW and DW were calculated from empirical data. Predictions regarding the whole water column (Fig. 3A) from all three models occurred within the uncertainty bands for all modelled years.

Predictions for the different water layers were less accurate compared to predictions concerning the whole water column. Mean annual TP in SW (Fig. 3B) was predicted within the uncertainty bands for the whole period in MW and DW (Fig. 3C and D) but beyond the uncertainty bands during some months in 2004 and 2007 in SW (Fig. 3B) with MeroLakeMab. Although the model was calibrated for 2004–2007 data and not for 2008 data, the model error for 2008 was not particularly conspicuous among the years displayed in Fig. 3. TP concentrations increased in 2008 compared to 2007 (Fig. 3) despite the substantial decrease in TP input (Table 2). The variability of TP in MW and DW was particularly great this year (Fig. 3C and D), which could be an effect of extraordinary meteorological or hydrological events. Predictions from LakeMab were poorer than those from MeroLakeMab and predictions from the

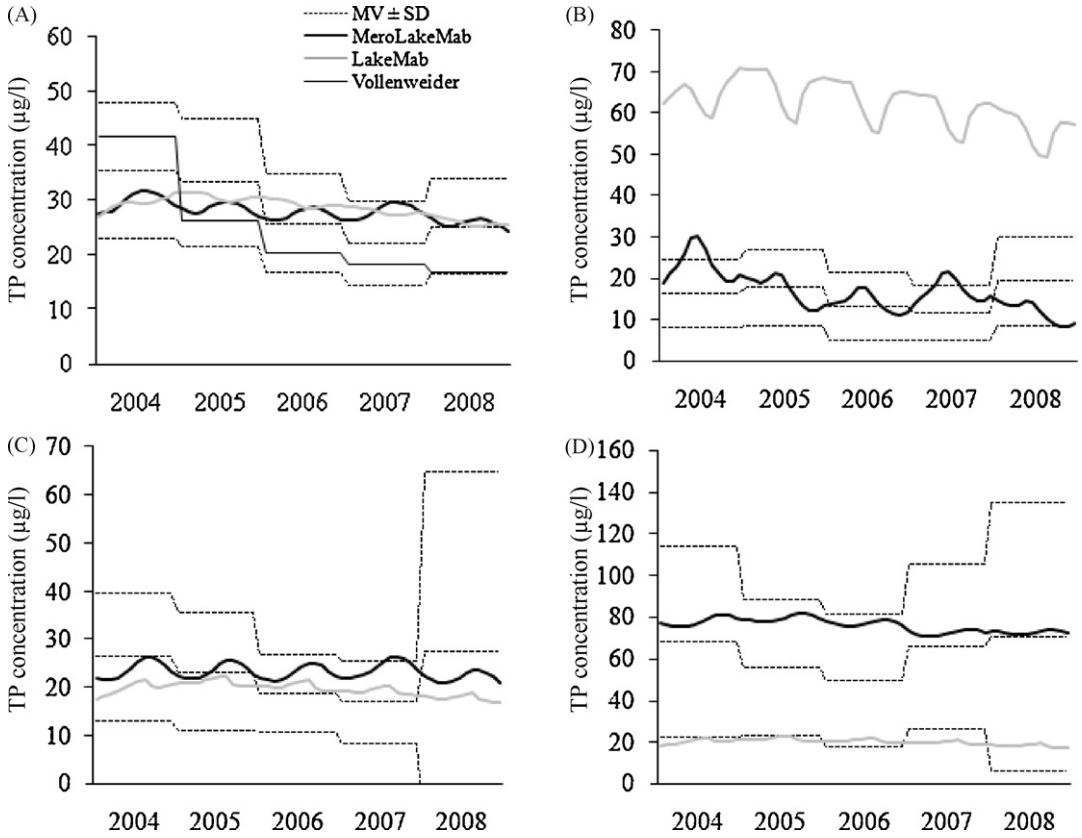

Fig. 3. Modelled and empirical TP concentrations in Lake Bourget for the period 2004–2008. (A) Whole water column, (B) surface waters, (C) middle waters, and (D) deep waters. Dashed lines (MV ± SD) denote mean annual values ± one standard deviation. Predictions from the MeroLakeMab, LakeMab and Vollenweider models are depicted with lines bearing the respective model name. The latter model is only suited for whole lake predictions and is therefore only included in (A).

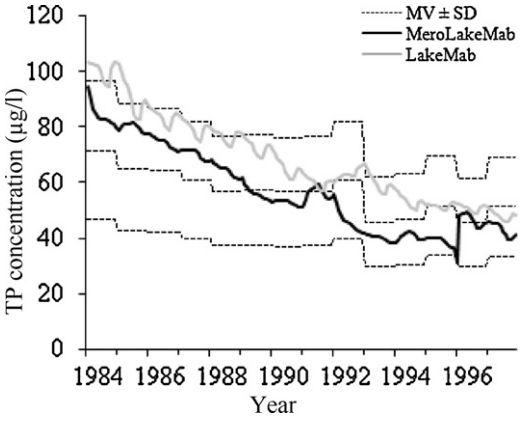

Fig. 4. Modelled and empirical TP concentrations in surface waters of Lake Lugano (N. basin), 1984–1997. Dashed lines (MV ± SD) denote mean annual values ± one standard deviation. Predictions from MeroLakeMab and LakeMab are depicted with lines bearing the respective model name.

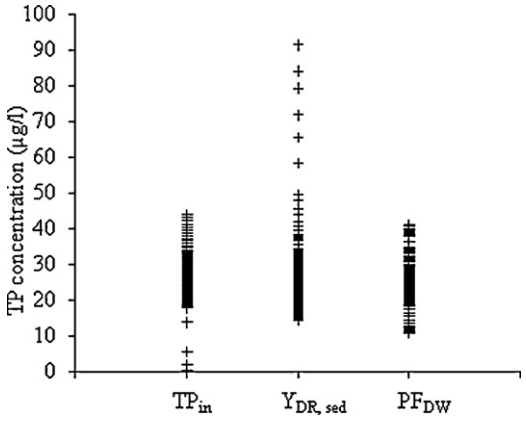

Fig. 6. Sensitivity analysis of the effect on lake TP concentrations from variations in TP concentrations in the tributaries (TP_{in}), the five sedimentation algorithms (F_{sed}) and PF_{DW} in Lake Bourget.

former of these models were encompassed by uncertainty bands for about two years in DW (Fig. 3D), five years in MW (Fig. 3C) but for none of the years in SW (Fig. 3B). LakeMab predicted higher TP concentrations in SW than in DW, which was not supported by empirical data.

Fig. 4 shows a time-series of yearly TP concentrations in surface waters or Lake Lugano's northern basin 1984–1997. Modelled concentrations from MeroLakeMab all appeared within the uncertainty bands, while some of the output data from LakeMab in the earliest part of the period exceeded data from Barbieri and Simona (2001) plus one standard deviation. Most of the output data from this model were, however, within the uncertainty bands.

TP concentrations from the whole water column and deep waters in 1996 are displayed in Fig. 5. For both of these water masses, MeroLakeMab apparently calculated concentrations that were lower than two given literature values, albeit within the uncertainty bands. LakeMab and the Vollenweider model yielded substantial underestimates (predictions from both models are represented by the grey line in Fig. 5A) of TP concentrations in the whole water column and LakeMab also underestimated the TP concentration in deep waters. A comparison between Figs. 4B and 3 give at hand that LakeMab predicted that concentrations would be much lower in deep waters than in surface waters in this lake as well as in Lake Bourget. Higher SW concentrations than DW concentrations could, however, not be empirically supported in either of the two investigated meromictic lakes.

Thus, the Vollenweider model provided poor predictions in Lake Lugano but good predictions in Lake Bourget. LakeMab yielded good TP predictions in the SW of Lake Lugano and good productions of whole-lake TP in Lake Bourget but provided an erroneous picture of the vertical TP distribution in both lakes. Figs. 3 and 5 demonstrated that although LakeMab may be useful for predicting trophic state changes in holomictic lakes (Bryhn and Håkanson, 2007), the model produced unacceptable predictions in both meromictic lakes of this study. Consequently, MeroLakeMab was chosen as a better alternative than the two other models for creating future scenarios and for estimating the TP loading history to Lake Bourget.

3.3. Sensitivity analysis for MeroLakeMab

Fig. 6 displays results from a Monte Carlo simulation analysis concerning the sensitivity of modelled TP concentrations in the whole water column of Lake Bourget. The Monte Carlo simulation was run with a stationary loading regime (at recent levels) of 30 tons TP per year. The sensitivity of modelled TP concentrations was analysed in relation to variations in (a) TP concentration in the inflow (C_{in}; in µg/l), (b) the dimensionless moderator $Y_{DR,sed}$ (dimensionless; see Eq. (12)), and (c) PF_{DW} (dimensionless). A variable (Rand; dimensionless) consisting of a normalised random series was created in the software Stella. The 100 positive values which were used from this series were normally distributed, had a mean value of 1 and a CV value of 0.4. All Rand values were consecutively multiplied with C_{in}, and the simulated lake TP concentration after 10 years (at stationary conditions) was recorded in each of the 100 runs. This procedure was subsequently repeated with the same Rand values multiplied by $Y_{DR,sed}$, and thereafter with Rand values multiplied by PF_{DW}. All other variables except for the investigated

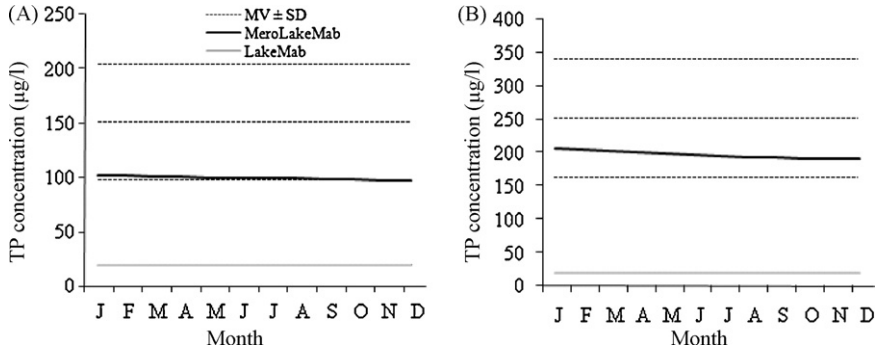

Fig. 5. Modelled and empirical TP concentrations in the whole water column (A) and bottom waters (B) of Lake Lugano (N. basin) in 1996. Dashed lines (MV ± SD) denote mean annual values ± one standard deviation. Predictions from MeroLakeMab and LakeMab are depicted with lines bearing the respective model name. Predictions from the Vollenweider model in (A) were very close to those from LakeMab and differences between output data from these two models cannot be visualised at the given scale.

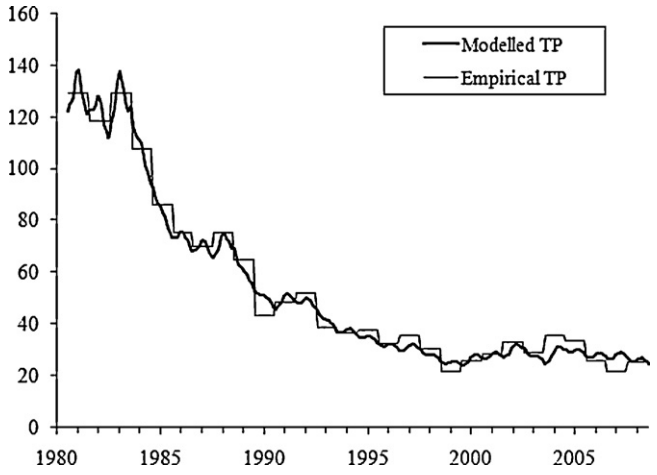

Fig. 7. Modelled TP concentrations (thick line) in Lake Bourget (whole water column; values in μg/l) compared to empirical annual values (thin line) 1981–2008.

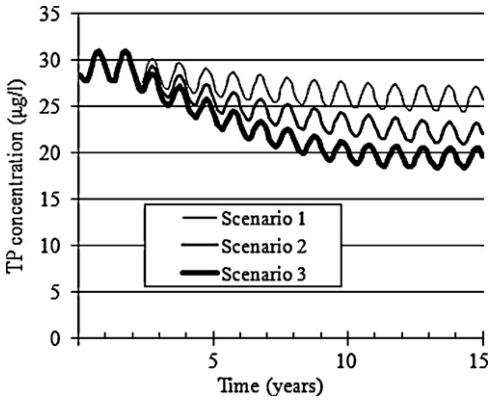

Fig. 8. Simulated decreases in TP loading in Lake Bourget. Scenarios: (1) a decrease in TP loading from 35 to 30 tons per year occuring in month 24 counted from the start of the simulation. Scenario 2: a decrease in TP loading from 35 to 25 tons per year occurring in month 24 counted from the start of the simulation. Scenario 3: a decrease in TP loading from 35 to 20 tons per year occuring in month 24 counted from the start of the simulation.

variable (C_{in}, followed by $Y_{DR,sed}$ and PF_{DW}) were kept constant. The resulting CV in lake TP concentration was 0.32 from variations in TP concentration in the inflow, 0.48 from variations in $Y_{DR,sed}$, and 0.31 from variations in PF_{DW}. This means that predictions were particularly sensitive to the uncertainty of the dimensionless moderator (Eq. (12)) applied on the sedimentation algorithms.

The sensitivity analysis connected to TP concentrations in tributaries also conveys that if we accept higher model uncertainties than 32% with respect to TP concentrations, we must accept an uncertainty in TP loading higher than 40%. As motivated in Section 2, the accepted model error in annual lake TP was 35%, so the modelled uncertainty in TP concentrations in tributaries can be approximated as $0.35/0.32 \times 0.4 = 44\%$. This figure was subsequently used in estimates of the TP loading.

3.4. Loading history and future scenarios

While winter TP concentrations in Lake Bourget have been measured on a regular basis since 1981, the TP loading history of Lake Bourget prior to 2004 is poorly known since TP in Rivers Leysse and Sierroz was not continuously monitored before this year. TP concentrations in lake water have been measured once or twice a month since November 1999, and a comparison between this time series (covering all seasons) and the longer series on winter concentrations gave at hand that yearly mean TP concentrations were generally 7.5% higher than winter concentrations. Annual mean TP concentrations are displayed in Fig. 7 together with modelled TP concentrations from MeroLakeMab.

The TP loading required to simulate the historical TP time series in Fig. 7 is given in Table 3. One can note that the loading in 1981–1984 may have been more than 8 times as high as in 1995–1999, although uncertainties are substantial, as demonstrated in the sensitivity analysis above and specified in Table 3. It is also worth noting that the loading in 1995–1999 (Table 3) may have been lower than in 2004–2007 (Table 2), although TP concentrations were slightly higher during 1995–1999 than in 2004–2007 (Fig. 7). The modelling showed that high TP concentrations in waters and sediments in 1995–1999 were to some extent remainders from the preceding decades with intensive TP loading, an observation which was supported by the sediment core analysis in Giguet-Covex et al. (2010).

Table 3
Model estimates of annual TP loading to Lake Bourget using MeroLakeMab.

Time period	Loading (tons/year)
1981–1984	256 ± 113
1985–1989	86 ± 38
1990–1994	34 ± 15
1995–1999	31 ± 13
2000–2003	36 ± 16

The three investigated scenario categories were (a) decreases in TP loading, (b) decreases in runoff and (c) temperature increases. Fig. 8 shows modelling results from MeroLakeMab simulating conditions in Lake Bourget during three different TP loading scenarios, all of which began with 24 months of TP loading corresponding to 35 tons per year, yielding lake TP concentrations around 29 μg/l (in agreement with recently measured values). After 24 months, the annual loading was decreased to 30, 25 or 20 tons in each of the respective scenario. After 8–10 years, the lake TP concentration stabilised around 26, 22 and 20 μg/l, respectively. The magnitude of seasonal variations in Fig. 8 was smaller than what the empirical data showed. Using the previously mentioned empirical conversion factor of 1.075 (yearly means divided by winter means), winter concentrations were calculated at approximately 24, 21 and 18 μg/l for the three different scenarios. It should be noted that these are estimates for average meteorological and hydrological conditions; during years with unforeseen changes in other external factors apart from the TP loading, such as particularly pronounced weather events, concentrations could differ considerably from these modelled values.

Results from the first set of climate change scenarios in which present and decreased runoff were simulated are illustrated in Fig. 9. The figure describes two typical annual cycles. Scenario 1 represented similar conditions to scenario 1 in Fig. 8 after 7–8 years, with runoff rates at present levels and a TP loading of 30 tons/year, which yielded lake TP concentrations near 26 μg/l. Scenario 2 included a 10% runoff decrease with the same TP loading as scenario 1, and TP concentrations evidently differed very little between these scenarios (Fig. 9). Scenario 3 described a 10% runoff decrease, but with the same TP concentration in tributaries as in scenario 1, i.e. a 10% decreased loading (to 27 tons/year), which would result in TP concentrations near 24 μg/l. In scenario 4, runoff was decreased by 20% but the loading remained at 30 tons/year, and Fig. 9 shows that lake TP concentrations from this scenario were very close to those from scenarios 1 and 2. Finally, scenario 5 was run to investigate effects from a 20% decrease in runoff, but with similar TP concentrations in the inflow as in scenario 1. This scenario thus decreased TP loadings by 20% (to 24 tons/year) compared to scenario 1 and Fig. 9 shows that lake TP concentrations decreased in this scenario to levels near 22 μg/l. This whole simulation exer-

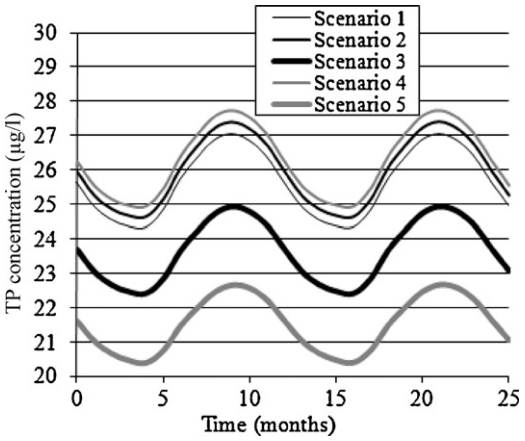

Fig. 9. Climate change scenarios describing long-term effects from changes in runoff on TP concentrations in Lake Bourget. Scenarios: (1) runoff rates corresponding to present rates. (2) A 10% decrease in runoff rates but similar TP loading as in scenario 1. (3) A 10% decrease in runoff rates but similar TP concentrations in tributaries as in scenario 1. (4) Same as scenario 2 but with a 20% runoff decrease. (5) Same as scenario 3 but with a 20% runoff decrease.

cise, illustrated in Fig. 9, suggested that decreases in water input to Lake Bourget at magnitudes forecasted by the IPCC (2007) would not affect TP concentrations *per se* to any notable extent. Marked changes in TP concentrations could, however, occur if decreases in runoff would significantly affect the TP loading.

The second set of climate change scenarios included changes in surface water temperatures by up to 4.5 °C and this set of scenarios is illustrated in Fig. 10. The TP loading was kept constant at 30 tons per year in all scenarios. One can note that the effects on yearly mean TP concentrations in the water column would be very modest compared to effects from changes in the TP loading (Fig. 8). A 4.5 °C temperature increase would increase the TP concentration by 4.6% (Fig. 10). At the beginning of the simulations (data not shown), temperature increases spurred an increase in sedimentation, which was followed by an increase in sediment diffusion of a slightly higher magnitude, and these mutually compensatory effects prevented any substantial impact on yearly mean TP concentrations in the water column. Simulations also suggested that the seasonal variation in concentrations would be less pronounced, as shown in Fig. 10, although it is important to bear in mind in this context that MeroLakeMab has been tested against annual mean concentrations and not in shorter time perspectives.

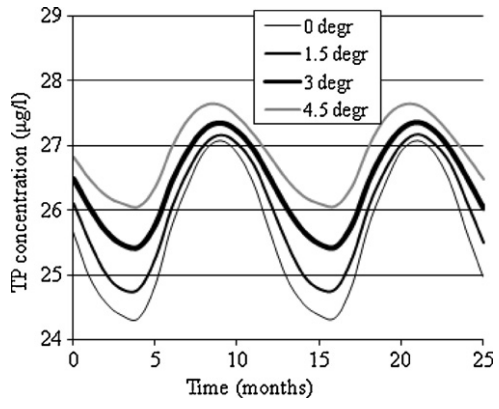

Fig. 10. Four scenarios on long-term effects from surface temperature increases in Lake Bourget.

4. Discussion and conclusions

This work presents the foundation for MeroLakeMab, a model which was constructed and tested against empirical data from two deep meromictic-like lakes. With the use of easily measurable driving variables and calibration constants that were valid for two different lakes, it was possible to circumvent some of the problems associated with lake-specific dynamic models described in Section 2. No weather data were necessary for driving the model, and the matrix of calibration constants in MeroLakeMab may be seen as more reliable than if the model output would have been tested against data from only one lake. However, extensive tests against a large number of other well-researched meromictic lakes would be required before MeroLakeMab can be described as having truly generic attributes.

The comparisons between modelled and empirical data revealed that LakeMab and the Vollenweider model were poorly suited to predict TP concentrations in the whole water column of Lake Lugano's northern basin, and also that LakeMab predicted several times higher TP concentrations in SW layers than in DW layers, which was contradicted by empirical data. Limitations in MeroLakeMab were instead that TP concentrations in SW and MW were sometimes predicted more than one standard deviation higher than empirical annual means in Lake Bourget, and that seasonal variations were not tested. However, these limitations may be considered as less discouraging than those of the other two models.

Apart from the introduction of two additional state variables (TP in deep waters and TP in deep A-sediments) for MeroLakeMab, there were some notable differences in sedimentation algorithms between this model and LakeMab, which need to be reflected on. These changes were necessary to sustain predicted TP concentrations in all of the three water layers close to empirical data from Lake Bourget and the northern basin of Lake Lugano. Fig. 6 showed that increases in the magnitude of the sedimentation algorithms may have a substantial impact on modelled TP concentrations in Lake Bourget, as increased sedimentation clears the waters from particulate P. Conversely, the low values for the particulate fraction in MW and DW (0.5 and 0.3, respectively; compared to 0.6 in SW), work in the opposite direction, i.e. low PF values decrease sedimentation and increase the TP concentration in the lake. We would, however, argue that it is reasonable to use lower PF values in the MW and DW layers than in SW for the following reasons: (1) SW is where the algal blooms occur, yielding extensive autochthonous particulate matter, (2) the sediment processes that primarily affect SW are erosion and resuspension of particulate matter (3) MW and DW are to a greater extent affected by diffusion of dissolved P from accumulation sediments. PF values as well as the dimensionless moderator for the sedimentation algorithms (Eq. (12)) which is based on the dynamic ratio could be investigated empirically in a cross-system study of a large number of meromictic lakes. Alternatively, the model assumptions motivated in this study, could be tested for a set of other well-researched meromictic lakes.

The sensitivity analysis (Fig. 6) also revealed that it is of great importance to have high accuracy in TP loading data. While this analysis certainly supports the conventional wisdom about the importance of TP loading accuracy for the success of lake eutrophication modelling (Håkanson, 1999), it also implies that reconstructions of loading histories must by necessity include substantial uncertainties. The estimates from Vinçon-Leite et al. (2002), a 50% loading decrease in the 1980s, are within the uncertainty bands of the results from this study, which instead indicated a 66% loading decrease between the early and late 1980s (Table 2). Likewise, the estimated 88% loading decrease between the early 1980s until the late 1990s should be interpreted using the uncertainties given in Table 3.

Fig. 7 shows that it is indeed possible to decrease TP concentrations further, although this would require additional efforts to decrease the TP loading. The estimates in Fig. 7 may provide useful information about what could be achieved after such efforts, as well as information about how long it would take until the full effect from abatement may be observed, i.e. as long as 8–10 years depending on the internal loading from sediments and the limited P exchange between water layers in meromictic lakes compared to holomictic lakes.

Blenckner et al. (2007) found a general, decreasing effect on winter and spring TP concentrations in lakes from climate change but no effects on summer TP concentrations, although it was stressed in their meta-analysis that any effects may vary from lake to lake depending on catchment area characteristics and differences in sediment-water dynamics. The climate change scenarios in the present study (Figs. 8 and 9) showed that the projected changes in runoff would only marginally affect TP concentrations in Lake Bourget. Temperature increases could have a slightly greater effect (a possible 4.6% increase in TP concentrations from a 4.5 °C increase in surface water temperature), although the discussed model uncertainties of up to 35% suggest that our projections associated with temperature increases should be interpreted with care. Both sedimentation and diffusion are spurred by increasing temperatures (Håkanson and Bryhn, 2008) and decreasing TP concentrations as suggested by Blenckner et al. (2007) would probably be more likely in shallow lakes where ET bottom types dominate and where diffusion is less important than in Lake Bourget. The greatest effects from climate change on TP concentrations in this lake would most probably occur if the TP loading would be significantly affected by changes in runoff or temperature.

Temperature increases may, however, have greater impact on biota than on TP concentrations. This could include improved competitive strength of temperature-dependent cyanobacteria as well as of daphnids and cyclopoid copepods (Blenckner et al., 2007; Jöhnk et al., 2008; Shatwell et al., 2008). Effects on these organisms and others from climate change are nonetheless difficult to predict because of the complexity of foodweb interactions in lakes (De Stasio et al., 1996) and it has been beyond the scope of this work to make such predictions for Lake Bourget.

To conclude, this study has presented a dynamic TP model which has been tested against empirical data from two meromictic-like lakes. This model was subsequently used to estimate that there has been an 88% decrease in TP loading to Lake Bourget between the early 1980s and the late 1990s. Climate change scenarios entailed only modest changes in TP concentrations from temperature increases or changes in runoff. A temperature increase would intensify P diffusion from deep sediments but would also increase P sedimentation and these two fluxes may have compensatory effects on the TP concentration. While climate change may pose a rather limited threat to Lake Bourget, it remains obvious from our results that changes in external TP loading have had, and may have, a massive impact on the ecosystem and that Lake Bourget still needs to be protected against extensive TP inputs, e.g., against erosion of P-rich material in the catchment.

Acknowledgements

We are grateful to all people involved in the survey of Lake Bourget and its catchment area for collecting and sharing data of interest for this paper. The authors are indebted to Jean-Marcel Dorioz, Jérôme Poulenard and Jérôme Lazzarotto for their critical comments to a previous version of the manuscript. Finally, comments from an anonymous reviewer have also greatly improved the final version of the paper.

Appendix A. Model equations

The dynamic model MeroLakeMab for meromictic lakes is based on the generic dynamic model LakeMab for holomictic lakes (for a motivation of its variables and constants, see Håkanson and Bryhn, 2008) and the adjustments made have been described and motivated in Section 2 of the present article. Water temperatures were predicted from altitude and latitude according to Ottosson and Abrahamsson (1998). General nomenclature for constants and variables: C = TP concentrations, D = depths or thicknesses, DC = distribution coefficients, F = TP fluxes, M = TP masses, Q = water fluxes, R = rates, T = time, t = time step (months), V = volumes, v = velocities, Y = dimensionless moderators. All of the variables, constants and equations below are illustrated in the supplementary material (Figs. S2–S15).

Obligatory lake-specific driving variables

Area [lake surface area, m^2]
$A_{catchment}$ [catchment area, m^2]
Alt [altitude, m.a.s.l; used in sub-models for temperature and water discharge]
C_{in} [flux-weighted TP concentration in tributaries, μg/l]
D_{max} [maximum depth, m]
D_m [mean depth, m]
Lat [latitude, °N]
Prec [annual precipitation, mm]
Q [mean annual water discharge, m^3/year]

Surface-water (SW) compartment

$M_{SW}(t) = M_{SW}(t - dt) + (F_{in} + F_{MWSWx} + F_{ETSW} + F_{prec} - F_{out} - F_{SWMW} - F_{SWET} - F_{SWMWx}) \cdot dt$
INIT $M_{SW} = V_{SW} \cdot 0.001 \cdot 100$
$F_{in} = (Q/12) \cdot Y_Q \cdot C_{in} \cdot 0.001$
F_{MWSWx} = if $V_{SW}/V_{MW} < 1$ then $M_{MW} \cdot R_{mix}$ else $M_{MW} \cdot R_{mix} \cdot V_{SW}/V_{MW}$
$F_{ETSW} = M_{ET} \cdot R_{res} \cdot (1 - V_d/3)$
$F_{prec} = C_{prec} \cdot Area \cdot Prec \cdot 0.001 \cdot 0.001/12$
$F_{out} = M_{SW} \cdot R_{out}$
$F_{SWMW} = (1 - ET) \cdot M_{SW} \cdot R_{sed,SW} \cdot PF_{SW} \cdot ((1 - DC_{res,SW}) + Y_{res} \cdot DC_{res,SW})$
$F_{SWET} = M_{SW} \cdot R_{sed,SW} \cdot PF_{SW} \cdot ET \cdot ((1 - DC_{res,SW}) + Y_{res} \cdot DC_{res,SW})$
$F_{SWMWx} = M_{SW} \cdot R_{mix}$

Middle-water (MW) compartment

$M_{MW}(t) = M_{MW}(t - dt) + (F_{SWMW} + F_{ETMW} + F_{SWMWx} + F_{MidAMW} + F_{DWMW} - F_{MWSWx} - F_{MWMidA} - F_{MWDW}) \cdot dt$
INIT $M_{MW} = V_{MW} \cdot 0.001 \cdot 140$
F_{DWMW} = if $(C_{DW} \cdot (1 - PF_{DW}) < C_{MW} \cdot (1 - PF_{MW}))$ then 0 else $M_{DW} \cdot R_{diff,DWMW} \cdot (C_{DW} \cdot (1 - PF_{DW}) - (C_{MW} \cdot (1 - PF_{MW}))$
$F_{ETMW} = M_{ET} \cdot R_{res} \cdot (V_d/3)$
$F_{MidAMW} = M_{MidA} \cdot R_{diff,MidA}$
$F_{MWMidA} = Y_{TMW,sed} \cdot M_{MW} \cdot R_{sed,MW} \cdot PF_{MW} \cdot ((1 - DC_{res,MW}) + Y_{res} \cdot DC_{res,MW}) \cdot MidA/(MidA + DeepA)$
F_{MWSWx} = if $V_{SW}/V_{MW} < 1$ then $M_{MW} \cdot R_{mix}$ else $M_{MW} \cdot R_{mix} \cdot V_{SW}/V_{MW}$
$F_{MWDW} = Y_{TMW,sed} \cdot M_{MW} \cdot R_{sed,MW} \cdot PF_{MW} \cdot ((1 - DC_{res,MW}) + Y_{res} \cdot DC_{res,MW}) \cdot DeepA/(MidA + DeepA)$
$F_{SWMW} = (1 - ET) \cdot (M_{SW} \cdot R_{sed,SW} \cdot PF_{SW} \cdot ((1 - DC_{res,SW}) + Y_{res} \cdot DC_{res,SW})$
$F_{SWMWx} = M_{SW} \cdot R_{mix}$

Deep-water (DW) compartment

$M_{DW}(t) = M_{DW}(t - dt) + (F_{MWDW} + F_{DeepADW} - F_{DWMW} - F_{DWDeepA}) \cdot dt$
INIT $M_{DW} = V_{DW} \cdot 0.001 \cdot 350$
$F_{MWDW} = Y_{TMW,sed} \cdot (M_{MW} \cdot R_{sed,MW} \cdot PF_{MW} \cdot (1 - DC_{res,MW}) + Y_{res} \cdot DC_{res,MW}) \cdot DeepA/(DeepA + MidA)$
$F_{DeepADW} = M_{DeepA} \cdot R_{diff,DeepA}$

F_{DWMW} = if (C_{DW} · (1 − PF_{DW}) < C_{MW}·(1 − PF_{MW})) then 0 else M_{DW}·$R_{diff,\ DWMW}$·(C_{DW} · (1 − PF_{DW}) − (C_{MW} · (1 − PF_{MW}))

$F_{DWDeepA}$ = $Y_{TDW,sed}$·(M_{DW} ·$R_{sed,\ DW}$·PF_{DW}·(1 − $DC_{res,MW}$) + Y_{res}·$DC_{res,MW}$)·DeepA/(DeepA + MidA)

ET-sediments

$M_{ET}(t)$ = M_{ET} (t − dt) + (F_{SWET} − F_{ETMW} − F_{ETSW}) · dt

INIT M_{ET} = 0.25·V_{ET} ·(1 − (W − 10)/100)·BD·1.3·1000

F_{ETMW} = M_{ET} · R_{res}·(V_d/3)

F_{ETSW} = M_{ET} · R_{res} · (1 − V_d/3)

F_{SWET} = M_{SW}·$R_{sed,SW}$ ·PF_{SW}·ET·((1 − $DC_{res,SW}$) + Y_{res}·$DC_{res,SW}$)

A-sediments below MW (MidA)

$M_{MidA}(t)$ = M_{MidA}(t − dt) + (F_{MWMidA} − F_{MidAMW} − $F_{bur,\ MidA}$) · dt

INIT M_{MidA} = V_{MidA} · (1 − W/100)·BD·1000

F_{MWMidA} = $Y_{TMW,sed}$·M_{MW}·$R_{sed,MW}$·(PF_{MW}·(1 − $DC_{res,MW}$) + Y_{res}·$DC_{res,MW}$)·MidA/(MidA + DeepA)

F_{MidAMW} = M_{MidA}·$R_{diff,MidA}$

$F_{bur,MidA}$ = M_{MidA}·(1.396/T_{MidA})

Deep A-sediments (DeepA)

$M_{DeepA}(t)$ = M_{DeepA}(t − dt) + ($F_{DWDeepA}$ − $F_{DeepADW}$ − $F_{bur,\ DeepA}$)·dt

INIT M_{DeepA} = V_{DeepA}·(1 − W/100)·BD·1000

$F_{DeepADW}$ = M_{DeepA}·$R_{diff,DeepA}$

$F_{bur,DeepA}$ = M_{DeepA}·(1.396/T_{DeepA})

$F_{DWDeepA}$ = $Y_{TDW,sed}$·M_{DW}·$R_{sed,DW}$·(PF_{DW}·(1 − $DC_{res,MW}$) + Y_{res}·$DC_{res,MW}$)·A_{DW}/(MidA + A_{DW})

Additional model variables

Amp_{MidA} = C_{MidA}·25 [amplitude value for A-sediments above D_{crit2}, dim. less]

Amp_{DeepA} = C_{DeepA}·25 [amplitude value for deep A-sediments, dim. less]

BD = 100·2.6/(100 + (W + IG·(1 − W/100))·(2.6-1)) [bulk density, g/cm^3]

BF_{DW} = if $Sedgram_{DeepA}$ > 400 then 1 else (1 + D_{Ased})$^{0.3}$ [bioturbation factor for deep A-sediments, dim. less]

BF_{MW} = if $Sedgram_{MidA}$ > 400 then 1 else (1 + D_{Ased})$^{0.3}$ [bioturbation factor for A-sediments above D_{crit2}, dim. less]

C_{DW} = 1000·M_{DW}/V_{DW} [TP concentration in DW, μg/l]

C_{DeepA} = M_{DeepA}/((V_{DeepA}·10^3·DeepA/(MidA + DeepA)·BD·(1 − W/100)) [TP-conc in deep A-sediments, mg/g dw]

C_{lake} = 1000·(M_{SW} + M_{MW} + M_{DW})/Vol [volume-weighted TP-conc in lake water, μg/l]

C_{MidA} = M_{MidA}/((V_{MidA}·10^3·MidA/(MidA + DeepA)·BD·(1 − W/100)) [TP-conc in deep A-sediments, mg/g dw]

C_{MW} = 1000·M_{MW}/V_{MW} [TP-conc in MW, μg/l]

C_{SW} = 1000·M_{SW}/V_{SW} [TP-conc in SW, μg/l]

$DC_{res,MW}$ = F_{ETMW}/(F_{ETMW} + F_{SWMW} + F_{MidAMW} + F_{DWMW} + F_{SWMWx}) [distribution coefficient for resuspended matter in MW, dim. less]

$DC_{res,\ SW}$ = F_{ETSW}/(F_{in} + F_{ETSW} + F_{prec} + F_{MWSWx}) [distribution coefficient for resuspended matter in SW, dim. less]

D_{crit1} = 45.7·√(Area·10^{-6})/(21.4 + √(Area·10^{-6})) [critical depth 1 in m, see Eq. (1)]

D_{crit2} = 6.70·$D_{max}$$^{1.23}$/(21.4 + √(Area·10^{-6})) [critical depth 2 in m, see Eq. (2)]

D_{DeepA} = if (D_{max} − D_{crit2})/2 < 1 then 1 else (D_{max} − D_{crit2})/2 [depth of deep A-sediments, m]

DeepA = 1 − ET-A_{MidA} [fraction of deep A-sediment areas, dim. less; Eq. (5)]

D_{ET} = D_{crit1}/2 [depth of ET-sediments, m]

D_{MidA} = if (D_{crit2} − D_{crit1})/2 < 1 then 1 else (D_{crit2} − D_{crit1})/2 [depth of A-sediments above D_{crit2}, m]

DR = √(Area·10^{-6})/D_m [dynamic ratio, dim. less]

ET = if ET1 > 0.95 then 0.95 else if ET1 < 0.15 then 0.15 else ET1 [fraction of ET-areas including boundary conditions, dim. less; see eq. 3]

ET1 = 1 − (D_{max} − D_{crit1})/(D_{max} + D_{crit1}· $e^{(3-Vd\hat{1}.5)}$)$^{(0.5/Vd)}$ [fraction of ET-areas without boundary conditions, dim. less, see Eq. (3)]

GS_{DeepA} = SMTH ($Sedgram_{DeepA}$, 60, $Sedgram_{DeepA}$) [gross sedimentation on deep A-areas, μg/cm^2·day]

GS_{MidA} = SMTH ($Sedgram_{MidA}$, 60, $Sedgram_{MidA}$) [gross sedimentation on A-areas above D_{crit2}, μg/cm^2·day]

IG = if W > 75 then (1280 + (W − 75)$\hat{3}$)/207 else W/11.9 [loss on ignition, %]

MidA = (1 − (D_{max} − D_{crit2})/(D_{max} + D_{crit2}·$e^{(3-Vd\hat{1}.5)}$))$^{(0.5/Vd)}$ −ET [fraction of A-sediments above D_{crit2}, dim. less; Eq. (4)]

MWT = [MW temperature, in °C; from temperature sub-model in Ottosson and Abrahamsson, 1998]

Q_{SWMW} = F_{SWMWx}/(C_{SW}·0.001) [water flux from SW to MW, m^3/month]

$R_{diff,DeepA}$ = $Y_{DR,diff}$·$Y_{TDW,diff}$·$R_{diff,default}$·$Y_{sed,DW}$·(DWT/4)·$Y_{TPDeepA}$ [diffusion rate from deep A-sediments, 1/month]

$R_{diff,MidA}$ = $Y_{DR,diff}$·$Y_{TMW,diff}$·$R_{diff,default}$·$Y_{sed,MW}$·(MWT/4)·$Y_{TP,\ MidA}$ [diffusion rate from A-sediments above D_{crit2}, 1/month]

R_{out} = 12·Q/V_{SW}·Y_Q·Y_{evap}·Y_{prec} [outflow rate, 1/month]

R_{res} = 1/T_{ET} [resuspension rate; 1/month]

$R_{sed,DW}$ = Y_{SPMDW}·$Y_{DR,sed}$·v/D_{DeepA} [sedimentation rate in DW; 1/month]

$R_{sed,MW}$ = Y_{SPMMW}·$Y_{DR,sed}$·v/D_{MidA} [sedimentation rate in MW; 1/month]

$R_{sed,SW}$ = Y_{SPMSW}·$Y_{DR,sed}$·v/D_{ET} [sedimentation rate in SW; 1/month]

$Sedcm_{DeepA}$ = $Sedgram_{DeepA}$·T_{dur}·10^{-6}·(100/(100 − W))·(1/BD) [mean annual deposition on deep A-sediments, cm/yr]

$Sedcm_{MidA}$ = $Sedgram_{MidA}$·T_{dur}·10^{-6}·(100/(100 − W))·(1/BD) [mean annual deposition on A-sediments above D_{crit2}, cm/yr]

$Sedgram_{DeepA}$ = $F_{DWDeepA}$·10^5/(30·2·Area·DeepA) [sedimentation on deep A-sediments, μg/(cm^2·day)]

$Sedgram_{MidA}$ = F_{MWMidA}·10^5/(30·2·Area·MidA) [sedimentation on A-sediments above D_{crit2}, μg/(cm^2·day)]

SPM_{DW} = 10$^{(1.56_log(CDW)-1.64)}$ [conc. of suspended particulate (SPM) in DW, mg/l]

SPM_{MW} = 10$^{(1.56_log(CMW)-1.64)}$ [SPM-conc in MW, mg/l]

SPM_{SW} = 10$^{(1.56_log(CSW)-1.64)}$ [SPM-conc in SW, mg/l]

SWT = [SW temperature, in °C; from temperature sub-model in Ottosson and Abrahamsson, 1998]

T = Vol/Q [theoretical water residence time, years]

T_{DeepA} = if 12·BF_{DW}·D_{Ased}/$Sedcm_{DeepA}$ > 3000 then 3000 elseif 12·BF_{DW}·D_{Ased}/$Sedcm_{DeepA}$ < 12 then 12 else 12·BF_{DW}·D_{Ased}/$Sedcm_{DeepA}$ [age of deep A-sediments, months]

T_{dur} = −0.058·Lat^2 + 0.549·Lat + 365 [duration of growing_season, days]

T_{DW} = M_{DW}/(F_{DWMW} + 0.001) [water residence time in DW, months; see Eq. (10)]

T_{ET} = if Y_{DR2} < 1 then 1 else Y_{DR2} [age of ET_sediments, months]

T_{MidA} = if 12·BF_{MW}·D_{Ased}/$Sedcm_{MidA}$ > 3000 then 3000 else if 12·BF_{MW}·D_{Ased}/$Sedcm_{MidA}$ < 12 then 12 else 12·BF_{MW}·D_{Ased}/$Sedcm_{MidA}$ [age of A-sediments above D_{crit2}, months]

T_{MW} = if V_{MW}/Q_{SWMW} > T·12/4 then T·12/4 else if V_{MW}/Q_{SWMW} < 0.5 then 0.5 else V_{MW}/Q_{SWMW} [water residence time in MW, months; Eq. (11)]

v = $v_{default}$·Y_{DR} [settling velocity of particles, m/month]

V_d = 3·D_m/D_{max} [form factor, dim. less]

V_{DeepA} = DeepA·Area·0.01·D_{Ased}·V_d/3 [volume of deep A-sediments, m^3]

V_{DW} = Area·DeepA·V_d·(D_{max} − D_{crit2})/3 [DW volume, m^3; Eq. (7)]

V_{ET} = ET·Area·0.01·D_{Ased}·0.1·V_d/3 [volume of ET-sediments, m^3]

V_{MidA} = MidA·Area·0.01·D_{Ased}·V_d/3 [volume of A-sediments above D_{crit2}, m^3]

V_{MW} = (Area·D_m − V_{SW} − V_{DW}) [MW volume, m^3; Eq. (8)]

Vol = Area·D_m [lake volume, m^3]

V_{SW} = Area · (D_m − (MidA + DeepA)·V_d·(D_{max} − D_{crit1})/3) [SW volume, m^3; Eq. (6)]

W = if DR > 6 then 65 else if DR > 0.5 then 75 else if DR > 0.045 then 85 else 95 [water content in A-sediments, %]
Y_{DR} = if DR < 0.26 then DR/0.26 else 0.26/DR [dimensionless moderator with boundary conditions for settling velocity]
$Y_{DR,\ diff}$ = if DR < 3.8 then 1 else 3.8/DR [dim. less moderator for diffusion from A-sediments]
$Y_{DR,\ sed} = 5.8 \cdot \sqrt{DR}$ [dim. less moderator for sedimentation; Eq. (12)]
Y_{DR2} = 12·DR/0.26 [dim. less moderator for T_{ET}]
Y_{evap} = if SWT < 9 then 1 else 1 − 0.4·(SWT/9-1) [dim. less moderator for evaporation]
Y_{prec} = if Prec < 650 then 1 + 1.8·(Prec/650-1) else 1 + 0.5·(Prec/650-1) [dim. less moderator for the effect of precipitation on outflow from lake]
Y_Q = [seasonal moderator for Q, from sub-model for water discharge in Håkanson and Bryhn, 2008]
$Y_{res} = T_{ET} + 10$ [dim. moderator for resuspension]
$Y_{sed,\ DeepA}$ = if GS_{DeepA} < 50 then (2-1·(GS_{DeepA}/50-1)) else (2 + Amp_{DeepA}·(GS_{DeepA}/50-1)) [dim. moderator for diffusion from deep A-sediments]
$Y_{sed,\ MidA}$ = if GS_{MidA} < 50 then (2-1·(GS_{MidA}/50-1)) else (2 + Amp_{MidA}·(GS_{MidA}/50-1)) [dim. moderator for diffusion from A-sediments above D_{crit2}]
$Y_{SPM,DW}$ = (1 + 0.75·(SPM_{DW}/50-1)) [dim. moderator for settling velocity in DW]
$Y_{SPM,MW}$ = (1 + 0.75·(SPM_{MW}/50-1)) [dim. moderator for settling velocity in MW]
$Y_{SPM,SW}$ = (1 + 0.75·(SPMSW/50-1)) [dim. moderator for settling velocity in MW]
$Y_{TDW,sed}$ = if DR > 0.26 then $\sqrt{(T_{DW}\cdot 365/12)}$ else $\sqrt{(T_{DW}\cdot 365/12\cdot DR/0.26)}$ [dim. moderator for sedimentation in DW]
$Y_{TDW,diff}$ = if $Y_{TDW,diff1}$ < 1 then 1 else $\sqrt{Y_{TDW,diff1}}$ [dim. moderator for diffusion from deep A-sediments]
$Y_{TDW,diff1}$ = if $T_{DW}\cdot 365/12 > 120\cdot(0.26/DR)$ then $120\cdot(0.26/DR)$ else $T_{DW}\cdot 365/12$ [boundary conditions for $Y_{TDW,diff}$]
$Y_{TMW,sed}$ = if DR > 0.26 then $\sqrt{(T_{MW}\cdot 365/12)}$ else $\sqrt{(T_{MW}\cdot 365/12\cdot DR/0.26)}$ [dim. moderator for sedimentation in DW]
$Y_{TMW,\ diff}$ = if $Y_{TMW,\ diff1}$ < 1 then 1 else $\sqrt{Y_{TMW,\ diff1}}$ [dim. moderator for diffusion from A-sediments above D_{crit2}]
$Y_{TMW,\ diff1}$ = if $T_{MW}\cdot 365/12 > 120\cdot(0.26/DR)$ then $120\cdot(0.26/DR)$ else $T_{MW}\cdot 365/12$ [boundary conditions for $Y_{TMW,\ diff}$]
$Y_{TPDeepA}$ = if C_{DeepA} < 0.5 then 0 else $C_{DeepA}(C_{DeepA} - 0.5)/2$ [dim. moderator for diffusion from deep A-sediments]
Y_{TPMidA} = if C_{MidA} < 0.5 then 0 else $C_{MidA}(C_{MidA} - 0.5)/2$ [dim. moderator for diffusion from A-sediments above D_{crit2}]

Model constants

C_{prec} = 5 [typical TP-conc in precipitation, μg/l]
D_{Ased} = 10 [typical depth of active A-sediments in lakes, cm]
DWT = 5.6 [typical DW temperature in Lake Bourget, °C]
PF_{SW} = 0.6 [particulate fraction in SW, dim. less]
PF_{MW} = 0.5 [particulate fraction in MW, dim. less]
PF_{DW} = 0.3 [particulate fraction in DW, dim. less]
$R_{diff,default} = 2.5\cdot 10^{-5}$ [default diffusion rate from A-sediments, 1/month]
$R_{diff,DWMW}$ = 0.008 [diffusion rate from DW to MW, 1/month]
R_{mix} = 0.00008 [mixing rate, 1/month]
$v_{default}$ = 6 [default settling velocity of particles, m/month]

Appendix B. Supplementary data

Supplementary data associated with this article can be found, in the online version, at doi:10.1016/j.ecolmodel.2010.02.013.

References

Aldenberg, T., Janse, J.H., Kramer, P.R.G., 1995. Fitting the dynamic lake model PCLake to a multi-lake survey through Bayesian statistics. Ecological Modelling 78, 83–99.
Barbieri, A., Simona, M., 2001. Trophic evolution of Lake Lugano related to external load reduction: Changes in phosphorus and nitrogen as well as oxygen balance and biological parameters. Lakes and Reservoirs: Research and Management 6, 37–47.
Beven, K., 2006. A manifesto for the equifinality thesis. Journal of Hydrology 320, 18–36.
Blenckner, T., Adrian, R., Livingstone, D.M., Jennings, E., Weyhenmeyer, G.A., George, D.G., Jankowski, T., Järvinen, M., Aonghusa, C.N., Nõges, T., Straile, D., Teubner, K., 2007. Large-scale climatic signatures in lakes across Europe: a meta-analysis. Global Change Biology 13, 1314–1326.
Boehrer, B., Schultze, M., 2008. Stratification of lakes. Reviews of Geophysics 46 (RG2005), 27.
Bryhn, A.C., 2009. A morphometrically based method for predicting water layer boundaries in meromictic lakes. Hydrobiologia 636, 413–419.
Bryhn, A.C., Håkanson, L., 2007. A comparison of predictive phosphorus load–concentration models for lakes. Ecosystems 10, 1084–1099.
Bryhn, A.C., Hessen, D.O., Blenckner, T., 2007. Predicting particulate pools of nitrogen, phosphorus and organic carbon in lakes. Aquatic Sciences 69, 484–494.
Chorus, I., Bartram, J. (Eds.), 1999. Toxic Cyanobacteria in Water: A Guide to their Public Health Consequences, Monitoring and Management. Routledge, London, p. 400.
De Stasio Jr., B.T., Hill, D.K., Kleinhans, J.M., Nibbelink, N.P., Magnuson, J.J., 1996. Potential effects of global climate change on small north-temperate lakes: physics, fish, and plankton. Limnology and Oceanography 41, 1136–1149.
Giguet-Covex, C., Arnaud, F., Poulenard, J., Enters, D., Reyss, J.-L., Millet, L., Lazzaroto, L., Vidal, O., 2010. Sedimentological and geochemical records of past trophic state and hypolimnetic anoxia in large, hard-water Lake Bourget, French Alps. Journal of Paleolimnology 43, 171–190.
Håkanson, 1999. Water Pollution—Methods and Criteria to Rank, Model and Remediate Chemical Threats to Aquatic Ecosystems. Backhuys, Leiden, 277p.
Håkanson, L., Bryhn, A.C., 2008. A dynamic mass-balance model for phosphorus in lakes with a focus on criteria for applicability and boundary conditions. Water, Air & Soil Pollution 187, 119–147.
Håkanson, L., Peters, R.H., 1995. Predictive Limnology. SPB, Amsterdam, 464p.
Håkanson, L., Blenckner, T., Malmaeus, J.M., 2004. New, general methods to define the depth separating surface water from deep water, outflow and internal loading for mass-balance models for lakes. Ecological Modelling 175, 339–352.
Hu, W., Jørgensen, S.E., Zhang, F., 2006. A vertical-compressed three-dimensional ecological model in Lake Taihu, China. Ecological Modelling 190, 367–398.
IPCC, 2007. Climate Change 2007: Synthesis Report. IPCC, Geneva, 104 p.
IPCC, 2008. Climate Change and Water. IPCC, Geneva, 210 p.
Jacquet, S., Briand, J.-F., Leboulanger, C., Avois-Jacquet, C., Oberhaus, L., Tassin, B., Vinçon-Leite, B., Paolini, G., Druart, J.-C., Anneville, O., Humbert, J.-F., 2005. The proliferation of the toxic cyanobacterium Planktothrix rubescens following restoration of the largest natural French lake (Lac du Bourget). Harmful Algae 4, 651–672.
Jacquet, S., Druart, J.-C., Perga, M., Girel, C., Paolini, G., Lazzarotto, J., Domaizon, I., Berdjeb, L., Humbert, J.-F., Perney, P., Laine, L., Kerrien, F., 2008. Water Quality Survey of Lake Bourget in 2007 (Suivi de la qualité des eaux du lac du Bourget pour l'année 2007). Report, 162 p (in French).
Janse, J.H., 2005. Model studies on the eutrophication of shallow lakes and ditches. Doctor's dissertation, Wageningen, 378 p (electronic version available).
Jeppesen, E., Søndergaard, M., Jensen, J.P., et al., 2005. Lake responses to reduced nutrient loading—an analysis of contemporary long-term data from 35 case studies. Freshwater Biology 50, 1747–1771.
Jöhnk, K., Huisman, J., Sharples, J., Sommeijer, B., Visser, P., Stroom, J., 2008. Summer heatwaves promote blooms of harmful cyanobacteria. Global Change Biology 14, 495–512.
Ottosson, F., Abrahamsson, O., 1998. Presentation and analysis of a model simulating epilimnetic and hypolimnetic temperatures in lakes. Ecological Modelling 110, 223–253.
Pers, B.C., 2005. Modeling the response of eutrophication control measures in a Swedish lake. Ambio 34, 552–558.
Sas, H. (Ed.), 1989. Lake Restoration by Reduction of Nutrient Loading: Expectations, Experiences, Extrapolations. Academia Verlag Richarz, St. Augustin, Germany, p. 497.
Schindler, D.W., Hecky, R.E., Findlay, D.L., Stainton, M.P., Parker, B.R., Patterson, M.J., Beaty, K.G., Lyng, M., Kasian, S.E.M., 2008. Eutrophication of lakes cannot be controlled by reducing nitrogen input: results of a 37-year whole ecosystem experiment. PNAS 105, 11254–11258.
Shatwell, T., Köhler, J., Nicklisch, A., 2008. Warming promotes cold-adapted phytoplankton in temperate lakes and opens a loophole for oscillatoriales in spring. Global Change Biology 14, 1–7.
Vinçon-Leite, B., Tassin, B., Druart, J.-C., 2002. Phytoplankton variability in Lake Bourget: phytoplankton dynamics and meteorology. Lakes & Reservoirs: Research and Management 7, 93–102.
Vollenweider, R.A., 1976. Advances in defining critical loading levels for phosphorus in lake eutrophication. Mem. Ist. Ital. Idrobiol. 12, 201–244.